Available online at www.sciencedirect.com
ScienceDirect
Journal of the European Ceramic Society 32 (2012) 175–184
www.elsevier.com/locate/jeurceramsoc

Synthesis of (α- and β-)Si_3N_4/Si_2N_2O into silicon particulate porous preforms by hybrid system CVI and direct nitridation

J.C. Flores-García [a], M.I. Pech-Canul [a,b,*], A.L. Leal-Cruz [c], J.C. Rendón-Angeles [a,b]

[a] *CINVESTAV IPN-Saltillo, Carretera Saltillo-Monterrey Km 13.5, Ramos Arizpe, Coahuila, México 25900, Mexico*
[b] *CINVESTAV IPN-Zacatenco, Programa Doctoral en Nanociencias y Nanotecnología, Av. Instituto Politécnico Nacional 2508, Col. San Pedro Zacatenco, Apdo. Postal 14-740, México 07360, D.F., Mexico*
[c] *Universidad de Sonora, Departamento de Ingeniería Química y Metalurgia, Rosales y Colosio S/N, Hermosillo Sonora, México 83200, Mexico*

Received 18 March 2011; received in revised form 30 July 2011; accepted 7 August 2011
Available online 25 August 2011

Abstract

An investigation on the microstructure and mechanical properties of Si/Si_3N_4/Si_2N_2O porous ceramic composites, synthesized in a multi-step approach via hybrid precursor system chemical vapor infiltration (HYSYCVI) and direct nitridation (DN) has been conducted. Particulate silicon porous preforms were infiltrated in subsequent stages S1-1, S1-2 (both at 1300 °C for 70 min in high purity nitrogen (HPN) using Na_2SiF_6 as solid precursor) and S2 (1350 °C for 120 min in ultra high purity nitrogen (UHPN)). Chemical reactions that account for the formation of Si_2N_2O and Si_3N_4 are proposed. Results show that the microstructure of the composites was influenced by atmosphere type and processing stage, affecting kind, morphology and size (including nanometric size) of nitrides formed. Porous composites (43% porosity) with modulus of rupture (MOR) ≈ 43 ± 3.5 MPa (evaluated in four-point bending tests) and elastic modulus (E) ≈ 29 GPa (determined by the pulse-echo ultrasonic method) are routinely obtained.

Keywords: A. Powders-gas phase reaction; B. Composites; D. Nitrides; E. Structural applications; HYSYCVI

1. Introduction

Owing to their excellent physicochemical and thermomechanical properties, silicon nitride (Si_3N_4) and oxynitride (Si_2N_2O) are two of the most attractive materials for the preparation of porous ceramic materials for a broad range of engineering applications, demanding high strength, low density, high surface area, high permeability, low specific heat and high thermal insulation. They offer excellent chemical resistance, high thermal properties and excellent oxidation resistance in a variety of environments, which make them suitable for structural and functional applications. It is evident that in the form of porous components these materials offer the potential to be used as refractories for molten metals, hot liquids and corrosive gases; lightweight structures; heat exchangers; hot gas and molten metal filters; support for catalysts; thermal insulation materials; filters for purification systems of air and water and Diesel Particulate Filters (DPF), and preforms for the manufacture of metal/ceramic (using further liquid metal infiltration) or dense ceramic/ceramic composites.[1,2] An inherent challenge to the preparation of such phases is the control of their composition, morphology and size (micron and nanometric). Due to the well-known characteristics and properties of nano-scale materials, the preparation of porous ceramic composites with nanometric phases becomes even more appealing. For instance, ceramic silicon nitride nanocomposites can enhance its fracture strength not only at room temperature but also at high temperatures, up to about 1500 °C.[3] It should be recognized that these properties can be significantly improved because of the superplasticity-like attributes of silicon nitride.[4] This fact can have an important impact in the costs associated to

* Corresponding author at: CINVESTAV IPN-Saltillo, Carretera Saltillo-Monterrey Km 13.5, Ramos Arizpe, Coahuila, México 25900, Mexico. Tel.: +52 844 4389600x9678; fax: +52 844 4389610.
E-mail addresses: martpech@hotmail.com, martin.pech@cinvestav.edu.mx (M.I. Pech-Canul).

0955-2219/$ – see front matter © 2011 Elsevier Ltd. All rights reserved.
doi:10.1016/j.jeurceramsoc.2011.08.006

machining, because the fabrication of complex near-net-shape components may become feasible.

Although there are several potential routes for the processing of Si_3N_4/Si_2N_2O composites, the reports in the related literature are scarce. For instance the multi-pass extrusion process has been used for the fabrication of porous Si_3N_4/Si_2N_2O bodies, using a nitridation process at 1400 °C in flowing N_2 gas for 20 h.[5,6] However, long processing times negatively influence important aspects such as practicality and cost, which cannot be neglected.

Traditionally silicon nitride powders are synthesized via three main routes, namely, nitridation of Si metal powders, carbothermic reduction of silica in N_2 gas, and vapor phase reaction of $SiCl_4$ or silane (SiH_4) with ammonia, by chemical vapor deposition (CVD).[7] The reaction of silicon powder with nitrogen gas is conducted at temperatures from 1250 to 1400 °C according to the reaction

$$3Si_{(s)} + 2N_2 \rightarrow Si_3N_{4(s)} \quad (1)$$

and generally consists of a 90:10 mixture of α-Si_3N_4 and β-Si_3N_4 polymorphs. The direct nitridation of silica in the presence of carbon and nitrogen takes place at temperatures between 1250 and 1550 °C according to the reaction

$$3SiO_{2(s)} + 6C_{(s)} + 2N_2 \rightarrow Si_3N_{4(s)} + 6CO_{(g)} \quad (2)$$

Usually both, the direct nitridation and the carbothermal reduction methods use seeds of Si_3N_4 powder mixed with the silicon to hasten the reactions.

The synthesis route for amorphous and crystalline α- and β-Si_3N_4 involving gas phase reactions, commonly referred to as chemical vapor deposition (CVD), typically starts from silicon gas precursors (silane and halides like $SiCl_4$, SiF_4, $SiBr_4$ and SiI_4) or silicon liquid precursors (metalorganics as tetra-methylsilane), and mainly from ammonia as nitrogen gas precursor.[7,8] During processing the liquid or gas precursors undergo decomposition into more reactive species that further interact to form Si_3N_4. Silane (SiH_4) and silicon tetrachloride ($SiCl_4$) are the most commonly used silicon precursors while ammonia is the most preferred nitrogen precursor.

Via CVD, high purity Si_3N_4 powders are produced according to the following typical reactions

$$SiCl_{4(g)} + 6NH_{3(g)} \rightarrow Si(NH)_{2(s)} + 4NH_4Cl_{(g)} \quad (3)$$

$$3Si(NH)_{2(s)} \rightarrow Si_3N_{4(s)} + 2NH_{3(g)} \quad (4)$$

$$3SiH_{4(g)} + 4NH_{3(g)} \rightarrow Si_3N_{4(s)} + 12H_{2(g)} \quad (5)$$

The reason why NH_3 is preferred over N_2, is because nitrogen is thermally and chemically more stable than ammonia, which results more difficult to dissociate. Specifically, while the ionization potential for N_2 is 15.576 eV, the corresponding value for NH_3 is 10.2 eV.[9] Consequently, the synthesis of Si_3N_4 using only N_2 (to obtain accordingly nitride deposits free of hydrogen), and conventional CVD systems with common silicon precursors has long been a challenging task.

One potential route for the preparation of porous bodies of silicon nitride and oxynitride composites with advantageous processing characteristics as compared to the conventional processing routes is the hybrid precursor system chemical vapor infiltration (HYSYCVI). Since the HYSYCVD (hybrid precursor system chemical vapor deposition) and HYSYCVI synthesis methods combine the use of gas (N_2, NH_3 and N_2–NH_3 mixes) and solid precursors (for instance, Na_2SiF_6), they are referred to as a hybrid precursor based methods. Some of the potential benefits of the proposed method, with respect to existing commercial and alternative routes are: (1) in situ processing, because the silicon gas species (SiF_4, SiF_3, SiF_2, SiF and Si) are formed in the same reactor where Si_3N_4 is produced; (2) versatility, because it allows synthesizing Si_3N_4 and Si_2N_2O with a variety of morphologies (whiskers/fibers, films/coatings and particles) and sizes, including nanometric phases; (3) silicon nitride and oxynitride can be produced without the use of seeds of these ceramic materials; (4) economic, because by taking advantage of the intrinsic thermal gradients within the tube reactor, the process allows to saving energy; (5) low-pressure process, because it is carried out at pressures slightly above to that of the atmospheric pressure; (6) since the silicon solid precursor (Na_2SiF_6) is stable and safe at room temperature, it is used as a safe-deposit compound for the silicon gas species; (7) the process offers the potential to produce Si_3N_4 and Si_2N_2O *in pure nitrogen* in a simple thermal gradient reactor.

In this work, the authors report on the processing, microstructural study, physical and mechanical properties of $Si/Si_3N_4/Si_2N_2O$ nitride porous ceramic composites using the HYSYCVI and DN (direct nitridation) methods. A multiple infiltration approach in successive stages and in different nitrogen atmosphere types using HYSYCVI and a direct nitridation stage, distinguishes this particular investigation.

2. Experimental procedures

2.1. Processing of $Si/Si_3N_4/Si_2N_2O$ composites via HYSYCVI and DN

The composites were prepared starting from 50% porosity cylindrical preforms (3 cm in diameter × 1.25 cm high) made out of silicon powders of 12.4 μm average particle size. The porous preforms were prepared by the uniaxial compaction of silicon particulates (Si_p) (the subscript p stands for particulate) in a hydraulic press at a pressure of 10,000 kPa. The porous preforms were processed in a hybrid system chemical vapor infiltration (HYSYCVI) reactor, which consists of a horizontal tube furnace (3.175 cm internal diameter × 76.2 cm long) with end-cap fittings, gas inlets (and outlets) to supply the nitrogen precursor as well as devices to controlling gas flow rate, pressure and process atmosphere. The inorganic salt sodium hexafluorosilicate (Na_2SiF_6) was used as the solid precursor during processing, prepared by the uniaxial compaction (pressure of 5000 kPa) of its powders in the form of cylindrical tablets (3 cm in diameter × 1.5 cm height). Both powders, Si_p and Na_2SiF_6, were supplied by *Sigma–Aldrich Inc.* The silicon particulate porous preforms were positioned within the alumina tube at the high temperature zone, while the Na_2SiF_6 compacts were placed in the low temperature zone (see Fig. 1).

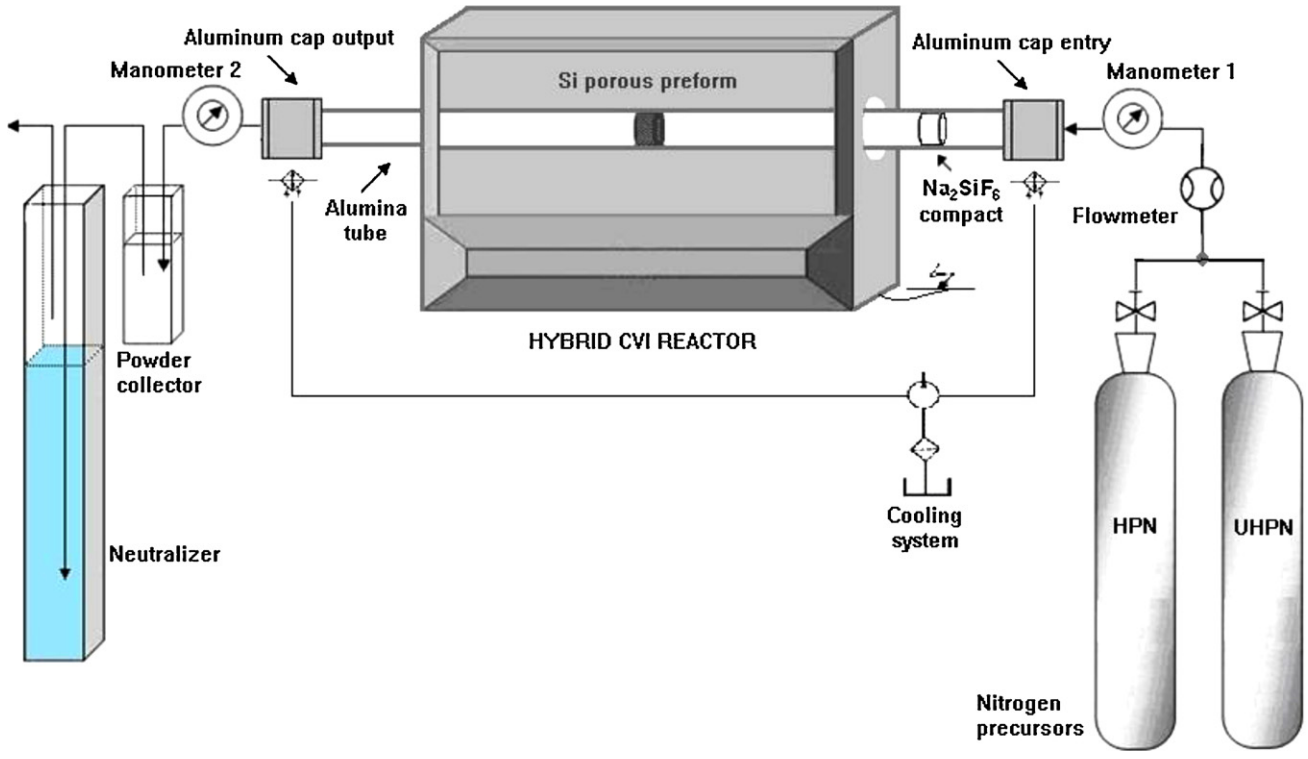

Fig. 1. Schematic representation of the experimental set-up.

The Si_p porous preforms were processed in the HYSYCVI reactor in subsequent stages S1 and S2. Stage S1 is carried out in two sub-stages (S1-1 and S1-2). The purpose of stage S1-1 was to trigger the formation of embryos of the nitrides (silicon oxynitride and nitride), while that of stage S1-2 was to promote phase growth. Stage 2, on the other hand, was conducted with the aim of conferring mechanical strength to the composites. As a whole, the processing in subsequent stages served as a means for a study of microstructural evolution. Each of the stages S1-1 and S1-2 consists of heating the Si_p porous preforms in high purity nitrogen (HPN) at a rate of 15 °C/min up to 1300 °C and then maintaining the specimen at this temperature for 70 min at a constant total pressure ($P_{total} = P_{atm} + P_{gage}$) of 102.64 kPa. During each sub-stage and simultaneously within the same reactor chamber, a compact of Na_2SiF_6 powders was heated (in the temperature range 543–565 °C) and decomposed to generate the silicon-fluorine (SiF_x, $x = 0$–4) gaseous reacting species necessary for the formation of silicon nitride (Si_3N_4) and oxynitride (Si_2N_2O), and their subsequent deposition on the substrate particles.[10] The temperature range for decomposition was determined from thermal analysis and from previous literature.[11] After the holding period of processing stage S1-1 the system was cooled down to room temperature in high purity nitrogen (HPN), after which the system was opened to remove the remaining of Na_2SiF_6 and the NaF formed. Then, a new Na_2SiF_6 compact was introduced for stage S1-2. After cooling down to room temperature, equally in HPN in stage S1-2, the system was opened to remove the remaining solid precursor and closed to conduct stage S2 in ultra high purity nitrogen (UHPN) and without the solid precursor. In stage S2 the samples were processed at a heating rate of 15 °C/min, maintained isothermally at 1350 °C for 120 min in UHPN at a flow of 30 cm^3/min, and maintaining the system at a constant pressure of 102.64 kPa. Table 1 summarizes the experimental conditions used in each of the processing stages.

After each stage of processing, the infiltrated specimens were analyzed by X-ray diffraction (XRD) and scanning electron microscopy (SEM). It should be noted that in previous investigations by the same research group, the processing conditions were used for only one infiltration step.[12] In order to establish chemical reactions for the phases formed, thermodynamic predictions using the FactSage™ program and databases were

Table 1
Parameters used during processing of $Si/Si_3N_4/Si_2N_2O$ porous composites.

Stage S1 (S1-1 and S1-2)[a]	
Processing temperature	1300 °C
Processing time	70 min
Nitrogen precursor	High purity nitrogen (HPN) N_2 99.997%
Flow rate of nitrogen precursor	15 cm^3/min
Quantity of Na_2SiF_6 (mass)	20 g
Stage S2	
Processing temperature	1350 °C
Processing time	120 min
Nitrogen precursor	Ultra high purity nitrogen (UHPN) N_2 99.999%
Flow rate of nitrogen precursor	30 cm^3/min
Constant conditions	
Total system pressure	102.64 kPa
Heating and cooling rate	15 °C/min

[a] Stage S1 consists of independent sub-stages S1-1 and S1-2, conducted subsequently.

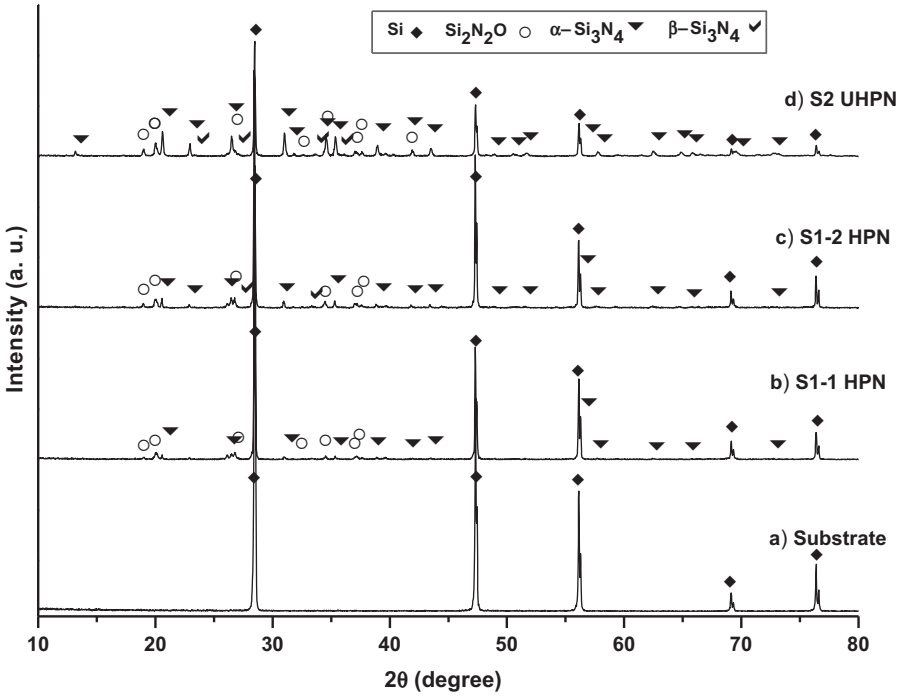

Fig. 2. X-ray diffraction patterns of Si specimens before and after successive stages of processing (S1-1 → S1-2 → S2) in HPN and UHPN.

conducted at the temperatures of 1300 and 1350 °C, and at a pressure of 1.013 atm. FactSage is the fusion of the FACT-Win/F*A*C*T and ChemSage/SOLGASMIX thermochemical packages. The FactSage package runs on a PC operating under Microsoft Windows® and consists of a series of information, database, calculation and manipulation modules that enable one to access and manipulate pure substances and solution databases. With the various modules one can perform a wide variety of thermochemical calculations and generate tables, graphs and figures of interest in several scientific fields of investigation.

2.2. Physical and mechanical property evaluation

The density (ρ_b) of the composites was determined by immersion in Hg using Archimedes' principle and confirmed via calculations based on the total volume (V_t) (dimensions measured with a Mitutoyo digital Vernier calliper) and weight determinations in an Explorer-Pro analytical scale. The percentage of infiltration (Inf. %) and porosity were determined by means of volume measurements in a He pycnometer at a constant helium (99.999%) calibration pressure of 0.117 MPa. In order to determine the modulus of rupture (MOR), four-point bending tests were carried out in a universal testing machine MTS model QTEST/100 with capacity of 100 kN, using a crosshead speed of 0.2 mm/s, in compliance with the ASTM C-1161-02 standard procedures, using configuration "A" specimens. The modulus of elasticity (E) was evaluated by means of non-destructive tests (based on the pulse and echo method), using a 5 MHz straight beam transducer (Panametrics Epoch IV ultrasonic equipment). The specimens were tested in agreement with the ASTM E 494-95 standard procedures.

3. Results and discussion

3.1. Specimen phase analysis and microstructure

X-ray diffraction patterns of specimens before and after the successive stages of vapor infiltration are shown in Fig. 2. Before the treatment, reflections pertaining only to the silicon (JCPDS-27-1402) particles are revealed. After processing, the presence of silicon nitride and oxynitride reflections – besides Si – is also observed. According to the analysis by XRD of processed specimens, Si_2N_2O (JCPDS-83-1853), α-Si_3N_4 (JCPDS-73-1210) and β-Si_3N_4 (JCPDS-71-0453) phases were formed on the Si_p porous preforms.

Results from phase semi-quantitative analysis by XRD show that in stage S1-1 (see Fig. 3) small amounts of Si_2N_2O and α-Si_3N_4 are produced and suggest that these phases served as embryos which then grew up in the subsequent stage S1-2. Although barely perceivable in Fig. 3, some β-Si_3N_4 was also formed in stage S1-2. Finally in stage S2, the increase in the amount of the three nitrides (Si_2N_2O, α- and β-Si_3N_4) is manifested. This semi-quantitative analysis showed a decrease in the silicon content in all processing stages, with a more evident decrease in the last stage. This is consistent with the decrease in the intensity of silicon reflections observed in the XRD patterns shown in Fig. 2. The crystallographic characteristics of the phases synthesized and used in the semi-quantitative analysis are shown in Table 2. The results show that in stage S1, formation of the three nitrides is governed by the HYSYCVI mechanism, while in stage S2, the direct nitridation (DN) mechanism operates, because in the last stage the solid precursor was not used any longer.

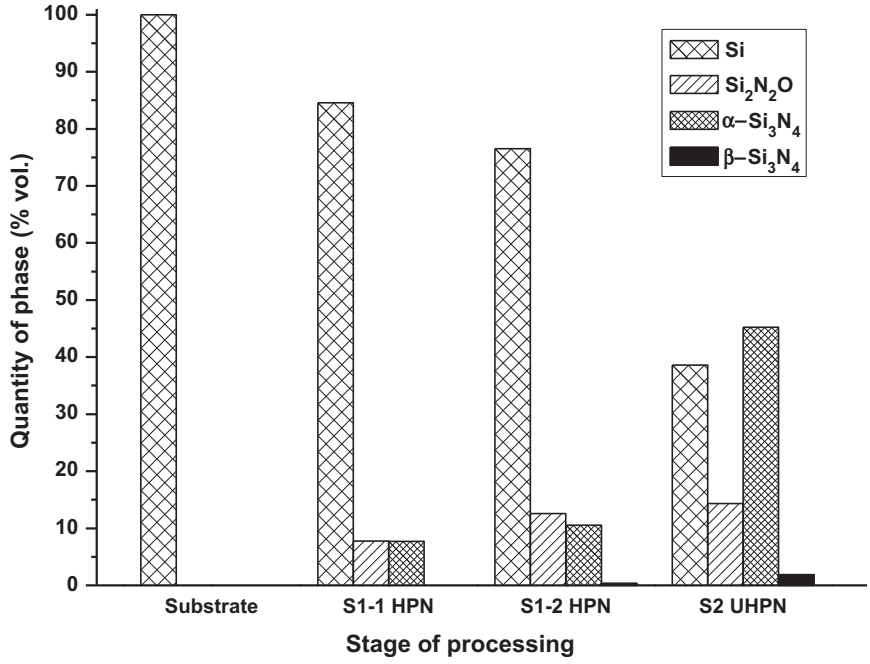

Fig. 3. Phase quantities into specimens processed in the successive stages of infiltration (S1-1 → S1-2 → S2) in HPN and UHPN.

Formation of the three nitrides can be explained in terms of gas phase and solid–gas reactions occurring in the system. And although several possible reaction pathways can be proposed to explain the appearance of the nitrides, essentially, they can be summarized in three mechanisms, which occur either independently or simultaneously, namely: (1) via gas phase reactions of the SiF_x species with the nitrogen precursor in stage S1; (2) via solid–gas reactions with the silicon particles: silicon particulate substrate direct oxynitridation and nitridation in stages S1 and S2; and (3) nitridation of Si_2N_2O phases already formed or the conversion from oxynitride to nitride by oxygen desorption. An analysis based on calculations using the FactSage™ program and databases is set forth as follows.

1. Via gas phase reactions of the SiF_x species with the nitrogen precursor in stage S1.

   This is assumed to occur through the reaction of Si–F_x species (evolved during the decomposition of Na_2SiF_6) with the N_2 and O_2 present in the system. In agreement with recent publications,[12,13] oxygen supplied in the nitrogen precursor plus the oxygen present in the reaction chamber is sufficient enough for inducing the formation of silicon oxynitride in the system. According to the gas supplier (INFRA) HPN and UHPN contain <10 ppm and <3.5 ppm O_2, respectively.

$$6SiF_{4(g)} + 6SiF_{3(g)} + 6SiF_{2(g)} + 6SiF_{(g)} + 6Si_{(g)} + 18N_{2(g)} + 3O_{2(g)} \rightarrow 6Si_2N_2O_{(s)} + Si_3N_4 + nNCP_{(g)} \quad (6)$$

$$\Delta G^{\circ}{}_{1300\,^{\circ}C} = -5176.35\,\text{kJ/mol}$$

where nNCP stands for moles of non-condensed phased (gaseous species formed or without reacting).

Eq. (6) corresponds to the maximum amount of silicon oxynitride formed. However, as the oxygen in the reaction chamber decreases with time, less oxynitride is formed, the amount of silicon nitride formed increases, and eventually both nitrides tend to equate:

$$6SiF_{4(g)} + 6SiF_{3(g)} + 6SiF_{2(g)} + 6SiF_{(g)} + 6Si_{(g)} + 18N_{2(g)} + 1.5O_{2(g)} \rightarrow 3Si_2N_2O_{(s)} + 3Si_3N_{4(s)} + nNCP_{(g)} \quad (7)$$

$$\Delta G^{\circ}{}_{1300\,^{\circ}C} = -4339.19\,\text{kJ/mol}$$

At longer periods of time – considering the depletion of oxygen – though relatively less thermodynamically feasi-

Table 2
Crystallographic data of the phases identified by XRD.

Phase	JCPDS ICDD No	Atomic structure	Most intense peaks and Miller indices (2θ) (h,k,l)
Si	27-1402	Cubic	28.443 (1,1,1); 47.304 (2,2,0); 56.122 (3,1,1)
α-Si_3N_4	73-1210	Hexagonal	35.339 (2,1,0); 20.60 (1,0,1); 31.008 (2,0,1)
β-Si_3N_4	71-0453	Hexagonal	27.048 (2,0,0); 33.632 (1,0,1); 36.041 (1,2,0)
Si_2N_2O	83-1853	Orthorhombic	20.00 (2,0,0); 26.447 (1,1,1); 18.989 (1,1,0)

ble, the amount of silicon nitride tends to outperform that of silicon oxynitride:

$$6SiF_{4(g)} + 6SiF_{3(g)} + 6SiF_{2(g)} + 6SiF_{(g)} + 6Si_{(g)} + 18N_{2(g)} \rightarrow 3Si_2N_2O_{(s)} + 5Si_3N_{4(s)} + nNCP_{(g)} \quad (8)$$

$$\Delta G^{\circ}{}_{1300\,^{\circ}C} = -3527.66\,kJ/mol$$

2. Via solid–gas reactions with the silicon particles: silicon particulate substrate direct oxynitridation and nitridation in stages S1 and S2:

$$4Si_{(s)} + 2N_{2(g)} + O_{2(g)} \rightarrow 2Si_2N_2O_{(s)} \quad (9)$$

$$\Delta G^{\circ}{}_{1300\,^{\circ}C} = -888.66\,kJ/mol$$
$$\Delta G^{\circ}{}_{1350\,^{\circ}C} = -861.57\,kJ/mol$$

The decrease of oxygen content in the reaction chamber results in the simultaneous formation of silicon nitride and oxynitride:

$$5Si_{(s)} + 3N_{2(g)} + \frac{1}{2}O_{2(g)} \rightarrow Si_2N_2O_{(s)} + Si_3N_{4(s)} \quad (10)$$

$$\Delta G^{\circ}{}_{1300\,^{\circ}C} = -676.85\,kJ/mol$$
$$\Delta G^{\circ}{}_{1350\,^{\circ}C} = -644.64\,kJ/mol$$

A last but less viable reaction is that for silicon nitride formation via direct nitridation of silicon:

$$3Si_{(s)} + 2N_{2(g)} \rightarrow Si_3N_{4(s)} \quad (11)$$

$$\Delta G^{\circ}{}_{1300\,^{\circ}C} = -232.52\,kJ/mol$$
$$\Delta G^{\circ}{}_{1350\,^{\circ}C} = -213.85\,kJ/mol$$

The ternary diagrams of condensed phase stability for the system Si–N_2–O_2 depicted in Fig. 4 – determined at 1300 and 1350 °C – shows thermodynamic stability regions in which it is possible to produce Si_3N_4 and Si_2N_2O together as stable solid phases under the test conditions specified in this work, confirming the occurrence of direct nitration reactions. Specifically, region III in the diagram confirms the feasibility of depositing silicon nitride and oxynitride together.

3. Nitridation of Si_2N_2O phases already formed or conversion from oxynitride to nitride by oxygen desorption, according to:

$$Si_2N_2O_{(s)} + 2N_{2(g)} \rightarrow -\infty Si_3N_{4(s)} + nNCP_{(g)} \quad (12)$$

$$\Delta G^{\circ}{}_{1350\,^{\circ}C} = -2.79\,kJ/mol$$

In Eq. (12) the symbol $-\infty$ indicates that the amount of Si_3N_4 phase is insignificant. Compared to the values of the Gibbs free energy change for the other reactions, the feasibility of reaction (12) is low; nonetheless, its occurrence has been suggested and demonstrated quantitatively in previous work.[13]

Considering mechanisms 1 and 2 at 1300 °C, it can be noted that it is more feasible the occurrence of gas phase reactions (Eqs. (6)–(8)) compared with solid–gas reactions (Eqs. (9)–(11)), which accounts for the behavior observed in stage S1. Referring to Fig. 3 once more, in stage S1-1, Si_2N_2O and α-Si_3N_4 are obtained in almost the same amounts but in stage S1-2, silicon oxynitride competes with alpha silicon nitride, and in the end, the former outperforms the latter. This is because – by comparison of the Gibbs free energy change for reactions (9)–(11)—it is easier to form oxide than non-oxide phases.[14] Formation of silicon oxynitride, α-Si_3N_4 and β-Si_3N_4 is mainly due to the reaction of Si–F_x species (generated by the decomposition of Na_2SiF_6) with the N_2 and O_2 present in the system according to the reactions proposed in Eqs. (1)–(3). It can also be attributed to the substrate direct nitridation and oxynitridation, because the presence of O_2 and N_2 can promote the direct reaction of the Si substrate as proposed through Eqs. (9)–(11) and Fig. 4.

The behavior observed in stage S2 can be explained by means of two possible mechanisms, namely, the direct nitridation and oxynitridation of silicon (Eqs. (9)–(11) and Fig. 4), and the oxygen desorption of the Si_2N_2O already formed (Eq. (12)), which corresponds to mechanisms 2 and 3. Two facts should be taken into account: (1) according to the experimental conditions used in stage S2 the nitrogen precursor contains less oxygen, and the temperature and time are higher than those used in stage S1, causing a decrease of the oxygen partial pressure in the system and giving rise to the formation of a larger amount of silicon nitride compared to oxynitride (see Eqs. (10) and (11)); (2) although Si_2N_2O is supposed to be a stable phase, under the experimental conditions, and, on account of the lower oxygen partial pressure in the nitrogen precursor, Si_2N_2O tends to undergo oxygen desorption and consequently, some α-Si_3N_4 could be formed (see Eq. (12)). This also allows inferring that the α polymorph of silicon nitride is formed first, compared to β-Si_3N_4. This seems to be the appearance order. According to thermodynamic calculations using the FactSage™ program and databases and because both nitrides (silicon nitride and oxynitride) are formed remarkably in the first stage, there can be no denying that the gas phase reaction in CVI is the main operating mechanism, although the direct nitridation reactions also take place during the formation of the nitrides. In the second stage, on the other hand, only direct nitridation reactions occur, due to the absence of the gas species (SiF_x) produced by the dissociation of the solid precursor Na_2SiF_6. A kinetics study would be required to elucidate the contribution of each of the mechanisms. Nevertheless, the kinetics study is beyond the scope of this work.

Since α-Si_3N_4 → β-Si_3N_4 transformation occurs at high temperature (≈1500 °C), it can be inferred that β-Si_3N_4 is formed via DN, although it is also evident that the HYSYCVI mechanism is a pre-requisite for the formation of beta silicon nitride. More detailed experiments would be required in order to elucidate its formation mechanism. It should be noted that

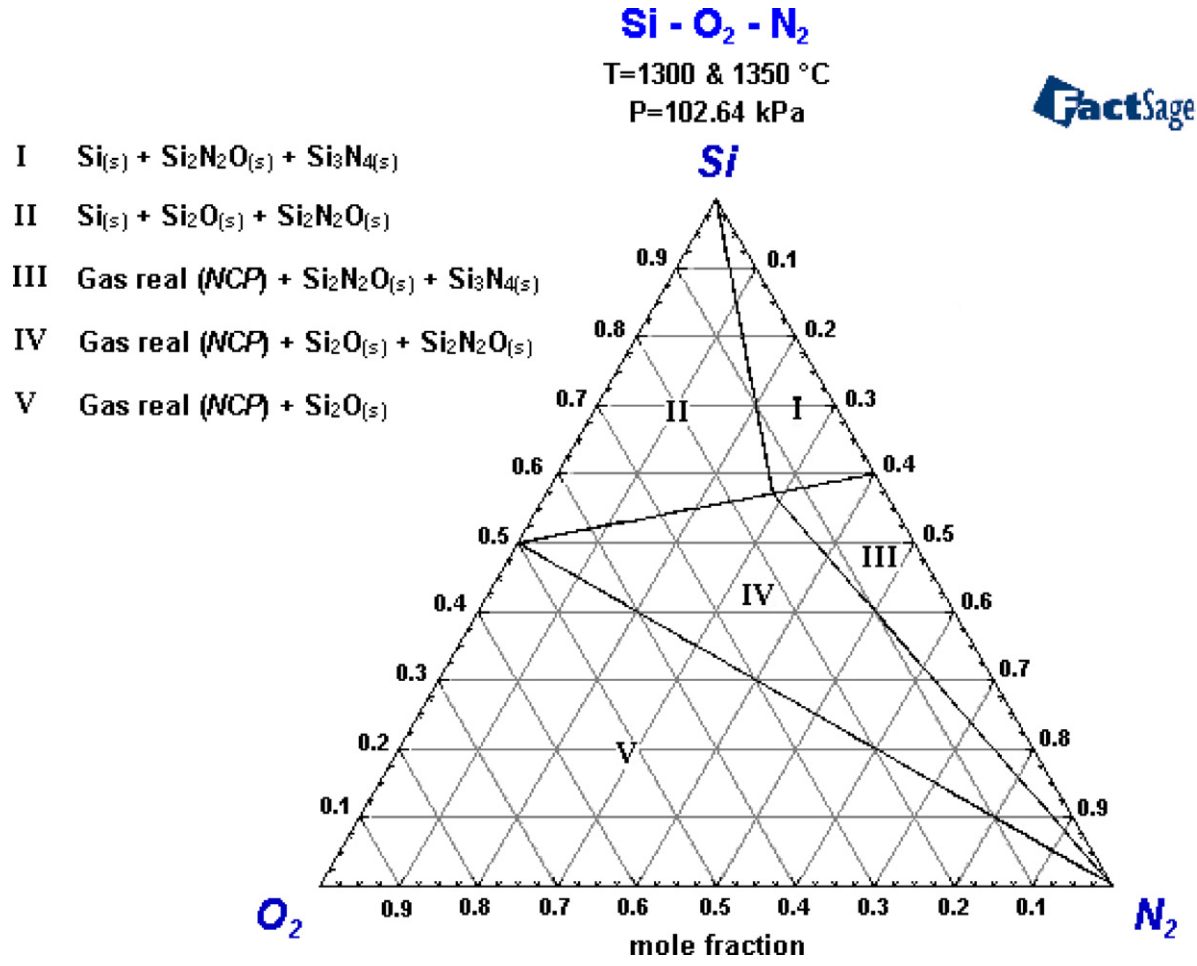

Fig. 4. Phase stability ternary diagram for the system Si–N_2–O_2.

the β phase of silicon nitride is stable and the most preferred polymorph.

Regarding the microstructural characterization, Figs. 5–8 show the results of SEM and EDS analyses of specimens before and after the processing in successive stages of infiltration. Fig. 5 shows the photomicrograph corresponding to the silicon particles, which have an irregular geometry and a wide particle size distribution, while the EDS analysis reveals the presence of silicon as the only element in the sample. Figs. 6 and 7 show representative photomicrographs of specimens processed in HPN in stages S1-1 and S1-2, respectively. Initially in stage S1-1 (Fig. 6), it can be seen that Si_2N_2O and α-Si_3N_4 deposits were formed on the Si substrate particles. These deposits show a sponge-like coating morphology featuring a growth of needle-like nanofibers with diameters from 100 to 400 nm and lengths up to about 5 μm. Afterwards, in stage S1-2 (Fig. 7), there is an increase in the amount of deposited phases that eventually form agglomerate compact deposits and fibrous

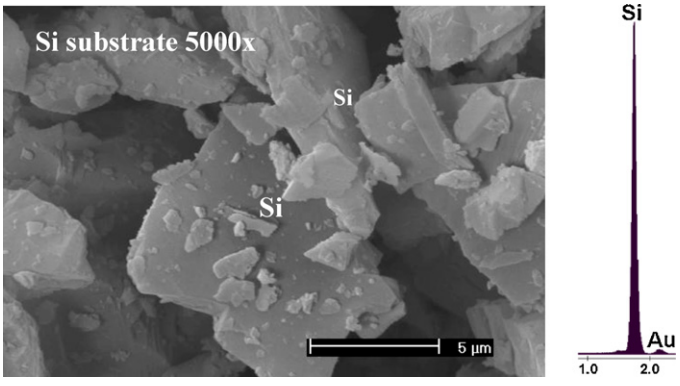

Fig. 5. SEM photomicrograph and EDS spectrum of Si porous preform before processing.

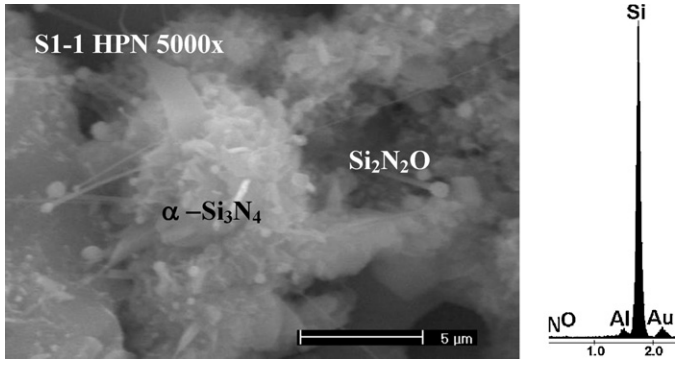

Fig. 6. SEM photomicrograph and EDS spectrum of Si specimen after processing in stage S1-1 in HPN.

Table 3
Physical characteristics of $Si/Si_3N_4/Si_2N_2O$ porous composites.

Specimen	Bulk density, ρ_b (g/cm^3)	Residual porosity, ε_r (%)	Infiltration (%)	Hg bulk density, ρ_{bHg} (g/cm^3)
$Si/Si_3N_4/Si_2N_2O$	1.5036	43.0999	6.900	1.4187

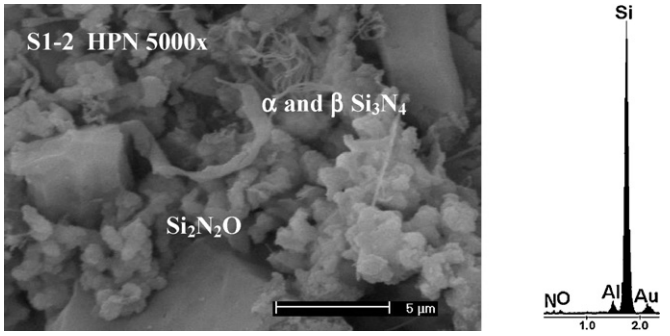

Fig. 7. SEM photomicrograph and EDS spectrum of Si after processing in stage S1-2 in HPN.

structures associated with the growth of Si_2N_2O, and α- and β-Si_3N_4.

Finally in stage S2, the change in the processing conditions mainly induced formation of α- and β-Si_3N_4 (see Fig. 8). Those phases exhibit a nano-cobweb morphology surrounding the composite and connecting silicon nitride agglomerates, as if the ramifications were grown up from the phases deposited in previous stages. The peaks corresponding to Si, N and O in the EDS spectra shown in Figs. 6–8, confirm the presence of the nitrides. An increase in the amount of nitrogen as the samples were processed – in agreement with the results from the semiquantitative analysis – can be observed. The variation in morphology, size and distribution of phases in the substrates processed at various processing stages and under different nitrogen atmospheres, as shown in the SEM analysis, can be attributed to both temperature and supersaturation condition (concentration of atoms or molecules adsorbed on the substrate surface).[15]

3.2. Physical and mechanical properties

Results from physical properties determination are summarized in Table 3. The bulk density exhibits an average value of 1.4612 g/cm^3 with a measurement error within 4% of that value, validated by the Archimedes' method and the geometric/volume approach. After the processing stage S2, the $Si/Si_3N_4/Si_2N_2O$ composites exhibit a residual porosity of ∼43%. This also indicates that the percentage of new phases formed is approximately 7%.

Results from the four-point bending tests indicate that the composites bear up an average maximum load of 10.5 ± 1.1 N. Under the assumption that the Si particulate porous preforms by themselves are not strong enough to bear up loads, the only way to explain the observed mechanical behavior is through the bonding effect of the new phases formed. Representative SEM photomicrographs of fractured surfaces of the composites, after the four-point bending tests support this postulation. The photomicrographs in Fig. 9(a) and (b) reveal an apparent reactivity of the Si particles if compared with the corresponding one (untreated Si) in Fig. 5. There is sufficient evidence in support of the chemical interaction of the Si particles to give place to new phases, namely, by the XRD results, by the thermodynamic predictions and by the microscopic examination, revealed in the photographs. Moreover, it can also be proposed that it is the fibers that link the particles and that after the fracture they look shorter, compared with the ones in Fig. 8.

Calculations of the modulus of rupture values obtained from the four-point bending tests indicate that the $Si/Si_3N_4/Si_2N_2O$ porous composites have an average flexural strength in of 43 ± 3.5 MPa. On the other hand, the results from the evaluation of Young's modulus (E)—determined via ultrasonic method, indicate an average value of 29 ± 1.6 GPa. Table 4 summarizes the magnitudes of the mechanical properties of the composites. It is interesting to note that despite the fact that the samples are porous and without sintering, the dispersions of the values of both, the MOR and E, are small. This is in good agreement with the homogeneous microstructure observed during the SEM analysis of fractured surfaces. However, several possible factors would account for the relatively modest magnitude of the MOR and explain the failure of the composites, namely: (i) regions of poor infiltration, (ii) segregation of particles or fibers of the new phases formed, (iii) agglomeration of particles due to inadequate compaction of the substrate preforms, (iv) detachment of particles during the preparation of the specimens, and (v) lack of full sintering. Fig. 10 shows representative images of fracture

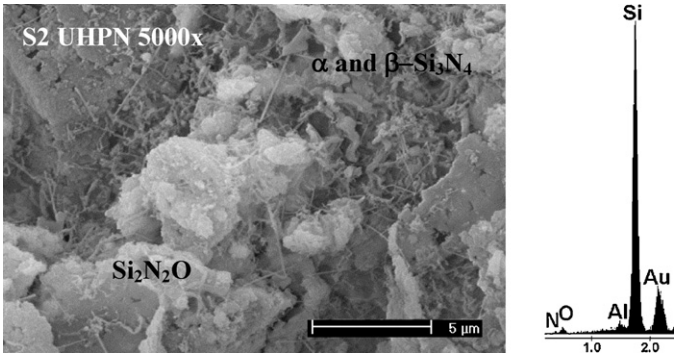

Fig. 8. SEM photomicrograph and EDS spectrum of Si specimen after processing in stage S2 in UHPN.

Table 4
Mechanical properties of $Si/Si_3N_4/Si_2N_2O$ porous composites.

Specimen	Average maximum load (N)	Modulus of rupture (MOR) (MPa)	Modulus of elasticity (E) (GPa)
$Si/Si_3N_4/Si_2N_2O$	10.5 ± 1.1	43 ± 3.5	29 ± 1.6

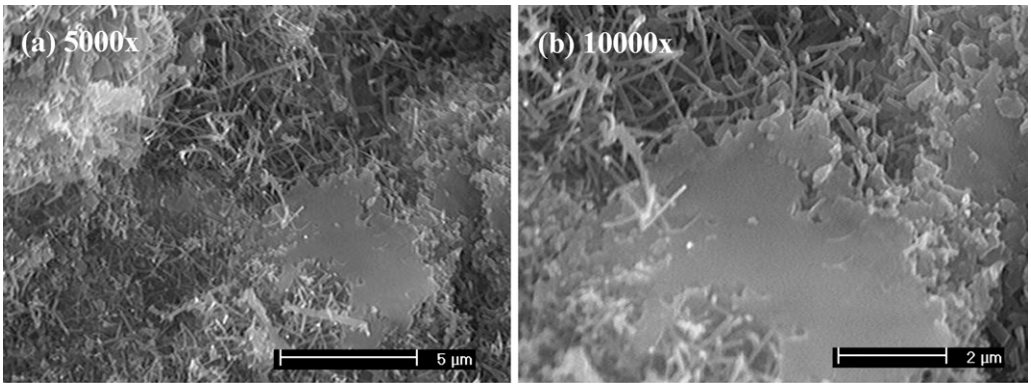

Fig. 9. SEM photomicrographs of fractured surfaces of the composites after the four-point bending tests.

surface of the composites evaluated in four point bending tests, taken at different magnifications. Fractographic analysis at low magnification (Fig. 10(a) and (b)) shows the good homogeneity of the sample, as a fine texture and regular porosity characterizes the material. Similarly, the typical images taken at medium magnifications (Fig. 10(c)) show that the filling of the interstices in the porous structure is uniform, which accounts for the moderate dispersion of the modulus of rupture. Given the fact that more alpha silicon nitride is obtained in stage S2, then, it would be reasonable to surmise that it is responsible for the mechanical behavior of the composites.

4. Summary and conclusions

The hybrid precursor system chemical vapor infiltration (HYSYCVI) route was used in a multi-step approach to synthesize micron- and nano-sized Si_3N_4/Si_2N_2O reinforcements into Si particulate preforms, producing $Si/Si_3N_4/Si_2N_2O$ porous composites. Characterization by XRD reveals that under the experimental conditions used Si_2N_2O, α-Si_3N_4, and β-Si_3N_4 phases were formed. According to the analysis by SEM, the Si_3N_4 and Si_2N_2O phases are deposited in a variety of morphologies, ranging from sponge-like coatings and nano pin-like fibers

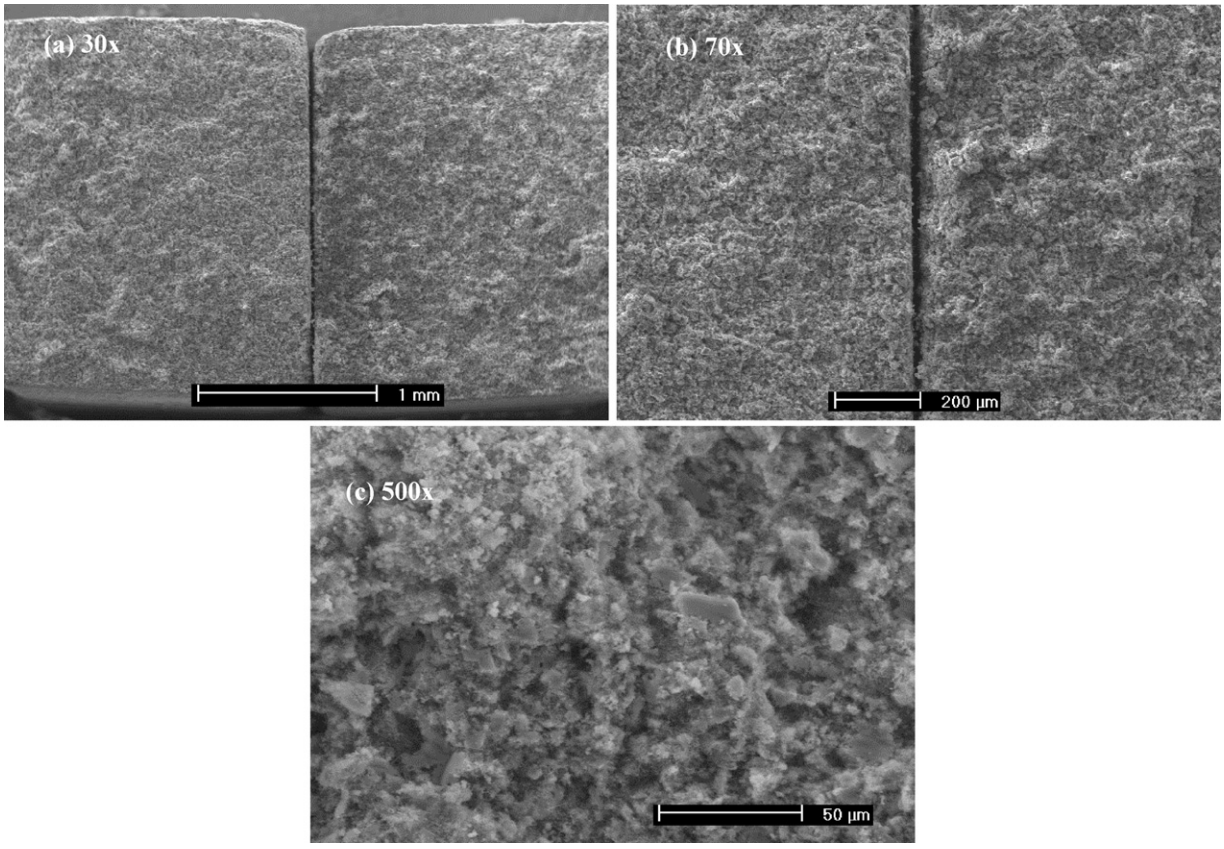

Fig. 10. Representative SEM photomicrographs of composites fracture surfaces taken at different magnifications.

to compact deposits and nano-cobweb morphology distributed into the composites. Thermodynamic predictions using the FactSage™ program and databases allowed proposing chemical reactions and ternary phase stability diagrams that account for the phases formed in the framework of the experimental conditions. The $Si/Si_3N_4/Si_2N_2O$ porous composites show effective porosities of ~43% after the processing in stages and an average bulk density of 1.4612 g/cm^3. They also exhibit an average modulus of rupture, with value of 43 ± 3.5 MPa and an average elastic modulus E of 29 ± 1.6 GPa. The mechanical properties obtained in this work are satisfactory enough to infiltrate the $Si/Si_3N_4/Si_2N_2O$ porous composites with liquid metals, for instance, for the production of Al MMCs, where the mechanical properties are expected to improve significantly. Nonetheless, results on that part of the work are beyond the scope of this paper.

Acknowledgements

Authors gratefully acknowledge CONACyT for financial support under contract No. SEP-CONACYT-2005-1/24322. Also, Mr. J.C. Flores-García expresses his gratitude to CONACyT for providing a scholarship. Finally, the authors also thank Mrs. M. Rivas-Aguilar and S. Rodriguez-Arias for technical assistance during the analysis by SEM and XRD, respectively.

References

1. Scheffler M, Colombo P. Cellular ceramics: structure, manufacturing, properties and applications. Weinheim: Willey-VCH Verlag GmbH & Co. KGaA; 2005.
2. Mujeebu MA, Abdullah MZ, Bakar MZ, Mohamad AA, Muhad RM, Abdullah MK. *J Environ Manage* 2009;**90**:2287–312.
3. Ajayan PM, Schadler LS, Braun PV. Nanocomposites science and technology. Federal Republic of Germany: Wiley-VCH Verlag; 2003.
4. Chen IW, Xue LA. Development of superplastic structural ceramics. *J Am Ceram Soc* 1990;**73**:2585–609.
5. Paul RK, Lee CW, Kim HD, Lee BT. Microstructure characterization of in situ synthesized porous Si_3N_4–Si_2N_2O composites using feldspar additive. *J Mater Sci* 2007;**42**:4701–6.
6. Lee BT, Paul RK, Lee CW, Kim HD. Fabrication and microstructure characterization of continuously porous Si_3N_4–Si_2N_2O ceramics. *Mater Lett* 2007;**61**:2182–6.
7. Lee WE, Rainforth WM. Ceramic microstructures property control by processing. London: Chapman and Hall; 1994.
8. Choy KL. Chemical vapour deposition of coatings. *Prog Mater Sci* 2003;**48**:57–170.
9. Weast RC. C.R.C. handbook of chemistry and physics. 51st ed. Cleveland, OH: The Chemical Rubber Co.; 1970.
10. Leal-Cruz AL, Pech-Canul MI. In situ synthesis of SiN_4 in the Na_2SiF_6–N_2 system via CVD: kinetics and mechanism of solid precursor decomposition. *Solid State Ionics* 2007;**177**:3529–36.
11. Leal-Cruz AL, Pech-Canul MI. In situ synthesis of Si_3N_4 from Na_2SiF_6 as a silicon solid precursor. *Mater Chem Phys* 2006;**98**(1):27–33.
12. Leal-Cruz AL. *Thermodynamics, kinetics and microstructural study of Na_2SiF_6 decomposition—silicon nitrides formation in systems Na_2SiF_6-nitrogen precursor-diluent*. Ph.D. Thesis, Mexico, Saltillo Coah Mexico: Cinvestav Saltillo; 2007.
13. Pech-Canul MI, De la Peña JL, Leal-Cruz AL. Effect of processing parameters on the deposition rate of Si_3N_4/Si_2N_2O by chemical vapor infiltration and the in situ thermal decomposition of Na_2SiF_6. *Appl Phys A* 2007;**89**:729–35.
14. De la Peña JL, Pech-Canul MI. Microstructure and kinetics of formation of Si_2N_2O and Si_3N_4 into Si porous preforms by chemical vapor infiltration (CVI). *Ceram Int* 2007;**33**:1349–56.
15. Blocher JM. Structure/property/process relationships in chemical vapor deposition CVD. *J Vac Sci Technol* 1974;**11**:680–6.